

CrossMark  
click for updatesCite this: *Anal. Methods*, 2015, 7, 4908

## Development of a resin based silica monolithic column encapsulation

Kara B. Spilstead,<sup>a</sup> Stephen J. Haswell,<sup>b</sup> Neil W. Barnett,<sup>a</sup> Xavier A. Conlan,<sup>a</sup> Paul G. Stevenson<sup>a</sup> and Paul S. Francis<sup>\*a</sup>

As monolithic columns become more extensively used in separation based applications due to their good flow and high surface characteristics, there has arisen the need to establish simple, reliable fabrication methods for fluidic coupling and sealing. In particular, the problem of liquid tracking between a monolith's outer surface and the sealing wall, resulting in poor flow-through performance, needs to be addressed. This paper describes a novel resin-based encapsulation method that penetrates 0.3 mm into the outer surface of a 4 mm diameter monolith, removing the so-called wall-effect. Results based on the peak analysis from 1  $\mu\text{L}$  of 0.4% thiourea injected into a 98 : 2 water : methanol mobile phase flowing at 1 mL  $\text{min}^{-1}$  indicate excellent flow conservation through the monolith. A comparison of peak shape and height equivalent to a theoretical plate (HETP) data between the reported resin-based method and the previously reported heat shrink tubing encapsulation methodology, for the same batch of monoliths, suggests the resin based method offers far superior flow characteristics. In addition to the improved flow properties, the resin casting method enables standard polyether ether ketone (PEEK) fittings to be moulded and subsequently unscrewed from the device offering simple reliable fluidic coupling to be achieved.

Received 18th March 2015

Accepted 30th April 2015

DOI: 10.1039/c5ay00722d

www.rsc.org/methods

## Introduction

Since their introduction in the early 1990s, the use of silica based monolithic rods as inert flow supports has grown substantially and they are now used in a wide range of applications, from catalysis through bioreactors to purification.<sup>1</sup> Their low backpressure flow characteristics and high surface areas make them particularly attractive for use in many applications, beyond their more traditional use in chromatographic based separations.<sup>2</sup> However, current encapsulation methods that fluidically seal monoliths and enable them to be connected or integrated into flow systems are still rather experimental and as a result, do not represent easy to use robust methodology.

Various encapsulation and interfacing methods for silica monoliths have been reported<sup>3–6</sup> but the most widely used encapsulation method, however, has been heat shrink polytetrafluoroethylene (PTFE) tubing,<sup>7,8</sup> due to its relative ease of use and connectivity. This approach however has been reported to give a poor seal with the outer monolith wall, allowing liquid to track between the tubing and the monolith, resulting in what is commonly known as the 'wall-effect'. As these wall-effects can reduce the performance of the various applications of

monoliths in fluidics systems, a more reliable encapsulation method is required. Whilst research has been conducted into the wall-effects in high performance liquid chromatography (HPLC) with particle packed columns (which is caused by radial heterogeneity with the packing),<sup>9</sup> little work has described the same effect with monolith structures.

In this paper we will describe a cost effective robust silica monolith encapsulation technique that not only overcomes unwanted wall-effects, but also enables direct fluidic connection to the monolith using standard union fittings.

## Experimental

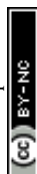
### Chemicals

The mobile phase for all HPLC analyses was a mixture of filtered (0.45  $\mu\text{m}$ ) deionised water (Continental Water Systems, Australia) and HPLC grade methanol (Scharlau, Gillman, South Australia, Australia) at a ratio of 98 : 2 water : methanol. Thiourea (BDH Chemicals, USA) was used as the test analyte, which was made to a concentration of 0.4% in the mobile phase solution.

Polystyrene casting resin and methyl-ethyl ketone peroxide catalyst (Recochem, Epping, Victoria, Australia) were purchased from a local hardware store. PTFE heat shrink tubing (4.8 mm  $\times$  1.2 m) was purchased from Element14 (Chester Hill, NSW, Australia). Monoliths were prepared in-house as described by Fletcher *et al.*<sup>7</sup> using Pluronic F127 polymer (Sigma-Aldrich), tetramethyl orthosilicate (TMOS) (Sigma-Aldrich) and 0.02 M acetic acid (Ajax Chemicals, Sydney, NSW, Australia).

<sup>a</sup>Centre for Chemistry and Biotechnology, School of Life and Environmental Sciences, Faculty of Science, Engineering and Built Environment, Deakin University, Geelong, Victoria, 3216, Australia. E-mail: paul.francis@deakin.edu.au

<sup>b</sup>Centre for Regional and Rural Futures, School of Life and Environmental Sciences, Faculty of Science, Engineering and Built Environment, Deakin University, Geelong, Victoria, 3216, Australia



## Equipment

Column efficiency tests were performed using an Agilent 1200 HPLC system (Agilent Technologies, Mulgrave, Victoria, Australia), consisting of a quaternary pump with solvent degasser, auto-sampler, and a diode array detection module that monitored the absorbance at 254 nm. Analysis was performed at room temperature. Data was obtained and processed with Agilent ChemStation software. Injections were 1  $\mu\text{L}$  and elution was performed under isocratic conditions at 1  $\text{mL min}^{-1}$ . Plate heights were calculated using the Foley–Dorsey equation using Wolfram Mathematica 10.1 (Hearn Scientific, South Yarra, Victoria, Australia). Microscope images were obtained using a Nikon Eclipse Ni-U Microscope, equipped with a DS-Qi2 16.25 Megapixel Monochrome Digital Camera (Scientific Equipment Pty Ltd, Huntingdale, Victoria, Australia). NIS Elements BR Basic Research Software (Scientific Equipment Pty Ltd, Huntingdale Victoria, Australia) was used to record resin penetration depth.

## Monolith fabrication

Monoliths were prepared using the method described by Fletcher *et al.*,<sup>7</sup> using Pluronic F127 polymer, 0.02 M acetic acid and TMOS as starting materials. Monoliths were moulded in a prefabricated acrylic mould, with a cylindrical shaft and conical ends, with final monolith dimensions of 50 mm  $\times$  4 mm. Monoliths were calcined in a furnace at 600  $^{\circ}\text{C}$  to remove organic material.

## Encapsulation methods

Before commencement of encapsulation, the resin was tested for solvent durability against a variety of commonly used HPLC solvents, including: acetonitrile, ethanol, heptane, isopropanol, methanol and tetrahydrofuran. It was found that only the acetonitrile had an impact on the resin, causing cracking and breakage, which occurred only after long exposure periods (24 h+) to undiluted acetonitrile. Thus, the polystyrene resin was deemed suitable for encapsulation, as the use of acetonitrile can often be substituted with methanol.

Moulds were constructed from 20 mL syringes (Terumo, Macquarie Park, NSW, Australia), lined with silicon mould release spray. The monolith was suspended between two HPLC polyether ether ketone (PEEK) finger-tight fittings (Sigma Aldrich), slotted inside rubber syringe plunger ends (see Fig. 1).

Approximately 20 mL of resin was combined with 15–20 drops of catalyst and stirred carefully with a flat spatula. The homogenous mixture was then poured over the suspended monolith until the monolith and fittings were well covered. Any bubbles were removed with a needle and syringe. Resin was allowed to set overnight in a fumehood before being removed from the mould. Fittings were unscrewed and replaced with the same fitting connected to capillary tubing (1/16" i.d.) and flow was tested by pumping coloured deionised water through the monolith.

Monoliths produced from the same batch were also encapsulated using a previously reported PTFE heat-shrink tubing

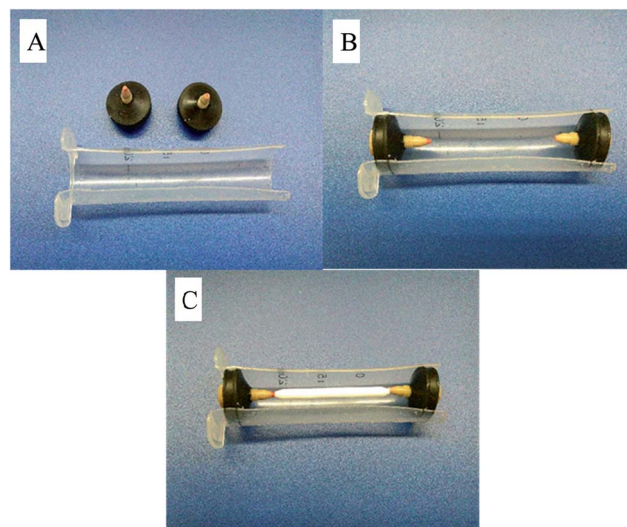


Fig. 1 Monolith encapsulation mould assembly. (A) Silicon release spray lined 20 mL syringe. (B) Rubber syringe ends in place, with HPLC fittings inserted. (C) Monolith suspended between HPLC fittings.

method<sup>9,10</sup> by inserting the monolith into a PTFE sleeve that was subsequently exposed to a heat gun at *ca.* 300  $^{\circ}\text{C}$  until shrinkage occurred around the monolith only. Steel HPLC tubing was then inserted and pushed flush with the ends of the monolith. Monolith and tubing were exposed to the heat gun until complete shrinkage had occurred and a tight seal formed around the monolith and tubing.

## Encapsulation method comparison

Both types of encapsulated monoliths were connected to the HPLC manifold to determine flow properties from the peak shapes generated. A flow rate of 1  $\text{mL min}^{-1}$  was employed, with 10 sequential injections of 1  $\mu\text{L}$  0.4% thiourea with a mobile phase of 98 : 2 water : methanol. This was repeated with pairs of columns from the same batch of monoliths encapsulated by the two methods described.

## Results and discussion

In order to assess the degree of resin ingress, encapsulated monolithic rods were cut in half with a saw revealing that the resin had penetrated the outer monolith surface by approximately 0.3 mm, as shown in Fig. 2. Penetration depth was measured using a calibrated Nikon Eclipse Ni-U Microscope (Scientific Equipment Pty Ltd, Huntingdale Australia) with built in measurement software (NIS Elements BR Basic Research Software, Nikon Instruments). This was repeated with several encapsulated monoliths, all of which showed similar penetration depths.

The observed resin penetration suggested that the wall-effects reported for the heat shrink encapsulation could be overcome using this method. Both the encapsulation methods were evaluated by comparing the peak shape generated from an injection of thiourea. This was repeated for three different pairs



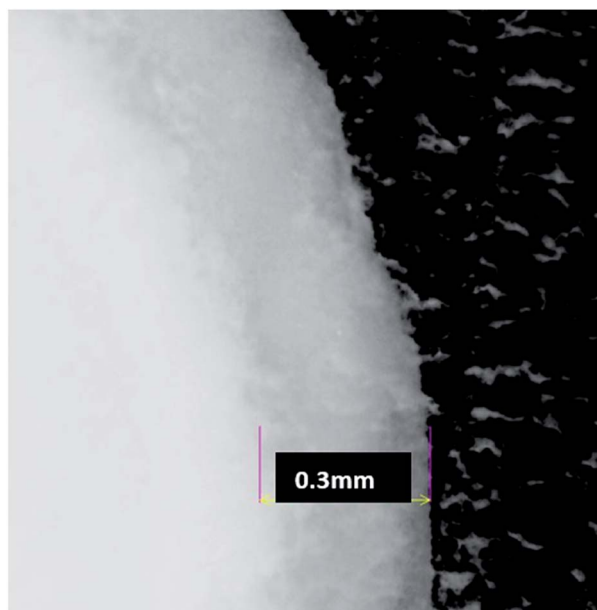


Fig. 2 Magnified image of resin encapsulated monolith. A clear grey band is distinctive between resin and monolith, where the resin has penetrated the monolith.

of monoliths encapsulated using the two methods described, the results for which are summarised in Table 1.

From the data in Table 1, it can be seen that the peak areas and RSDs for both types of encapsulation gave reasonable reproducibility within and between the batches of monoliths. The higher peak heights and symmetry of the resin encapsulated monoliths, however, demonstrate that the resin encapsulation method produced sharper peaks, alluding to the lack of distortion caused by wall-effects.

From Fig. 3, it can be seen that better peak shapes were achieved using the resin encapsulation method, suggesting that all the solution is flowing through the column, as opposed to some tracking around it, as is the case when wall-effects are present. The irregular shaped peaks, and peak fronting and tailing achieved using the shrink tubing encased monolith are common distortions in relation to wall-effects, where some of the solution has been eluted much faster than normal, due to a lack of resistance between the outside of the monolith and the

Table 1 Comparison of peak information between three pairs of monoliths encapsulated in the two described methods

Monolith pair	$t_R$ (min)/% RSD	Peak area/% RSD	Peak height	Symmetry
<b>Shrink tubing</b>				
1	0.4/16	6163/6.0	176	0.4
2	0.4/20	5813/2.0	275	0.5
3	0.4/12	5937/2.2	325	0.6
<b>Resin</b>				
1	0.5/1.1	5713/1.2	514	0.7
2	0.2/2.9	5962/3.0	787	0.3
3	0.3/0.8	6083/1.5	834	0.4

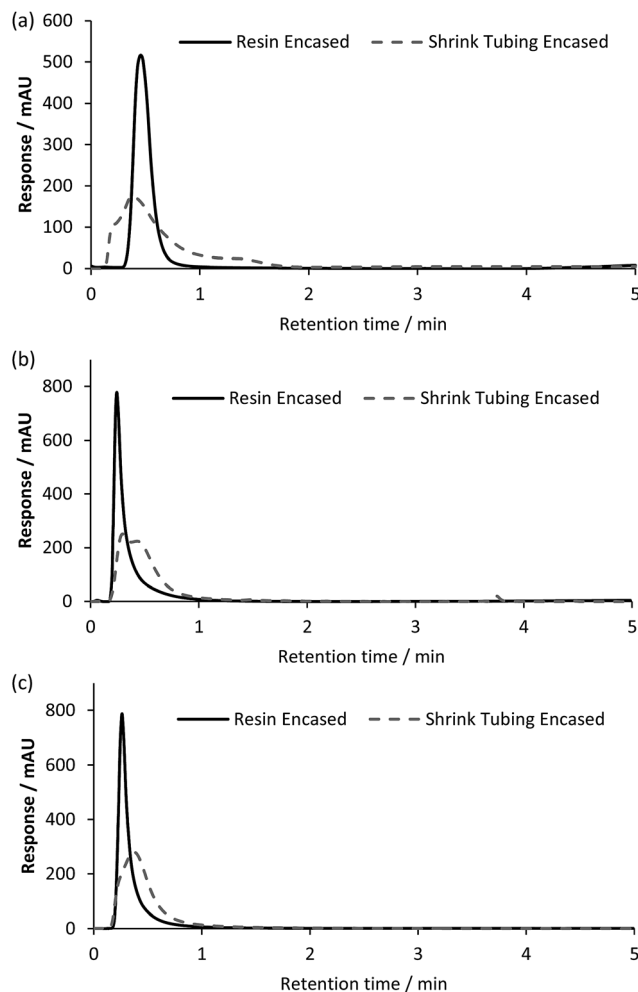


Fig. 3 (a) Pair 1. (b) Pair 2, (c) Pair 3. Mobile phase: 98/2 water/methanol. Flow rate:  $1 \text{ mL min}^{-1}$ .  $1 \mu\text{L}$  injections of 0.4% thiourea in mobile phase.

tubing wall. The split peaks observed with the shrink tubing encapsulated monoliths are most likely caused by the elution of a volume that flowed around the monolith, shortly followed by another volume eluted from inside the monolith. Moreover, in Fig. 3a, the extension of the peak to almost two minutes may be due to some of the analyte being eluted slower, potentially due to a void between the tubing and column inlet (eddy current), whereby the analyte is held and slowly bleeds into the monolithic bed. This phenomena was only observed with the shrink wrap method of encasement suggesting the resin method proposed was more effective at sealing in, and interfacing with the monolithic bed.

### HETP calculations

Height equivalent to a theoretical plate (HETP) was calculated for the above chromatograms to compare the efficiency of the two encapsulation methods. The number of theoretical plates ( $N$ ) was calculated with the Foley–Dorsey equation.<sup>10</sup> The results summarised in Table 2 show much smaller HETP values for the resin encapsulated monolith, which supports the data for peak



Table 2 *N* and HETP values (in mm) of the comparative pairs of monoliths encapsulated in resin versus heat shrink tubing

Monolith pair	Resin		Shrink tubing	
	<i>N</i>	HETP	<i>N</i>	HETP
1	53.3	0.09	2.31	2.16
2	21.8	0.23	5.66	0.88
3	48.1	0.10	9.62	0.51

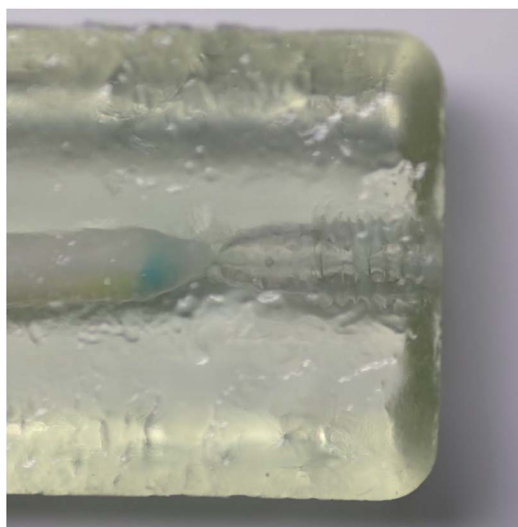


Fig. 4 Encapsulated monolith demonstrating fluid connectivity. Fittings have been removed. Monolith aligns with HPLC fitting port for matched alignment during each use.

shape and confirms more preferable flow characteristics. This is also evident from the chromatograms, Fig. 3, where the smaller plate height values correspond to a narrower peak.

The calculated plate heights for resin encapsulation are around 5–10 times larger than those of reported values for unmodified commercial silica monoliths;<sup>11</sup> and 20–100 times for those in heat shrink tubing.

### Fluidic connectivity

As indicated earlier, when the monoliths are cast in resin a PEEK connector is contact mounted at each end of the monolith (see Fig. 1 and 4), which can be unscrewed after curing and refitted with tubing connected. This provided a simple leak-proof low-volume interface to and from the monolith, as can be seen in Fig. 4.

## Conclusions

This encapsulation method offers a simple, low-temperature fluid-tight methodology for incorporating monoliths into flow systems. The relative symmetry of the unretained peak and lack of any other obvious detrimental wall-effects (chemical or fluidic), suggests that the monolith resin encapsulation method described is more reliable and superior in fluidic control and process efficiency than the previously reported heat shrink tubing encapsulated methodology. The encapsulation method was also found to offer a reliable and convenient way to connect flow fittings to the monoliths with minimal dead volume effects.

## Acknowledgements

The authors would like to thank Deakin University and the Australian Research Council (DP140100439) for funding this research; and Miss Jessica Learey for her design input.

## Notes and references

- 1 *Monolithic Silicas in Separation Science: concepts, syntheses, characterisation, modeling and applications*, ed. K. K. Unger, N. Tanaka and E. Machtejevas, Wiley-VCH Verlag mbH & Co. KGaA, Weinheim, 2011.
- 2 *Handbook of Solid Phase Microextraction*, ed. J. Pawliszyn, Elsevier, 2010.
- 3 S. Miyazaki, M. Takahashi, M. Ohira, H. Terashima, K. Morisato, K. Nakanishi, T. Ikegami, K. Miyabe and N. Tanaka, *J. Chromatogr. A*, 2011, **1218**, 1988–1994.
- 4 K. Cabrera, D. Lubda, H.-M. Eggenweiler, H. Minakuchi and K. Nakanishi, *J. High Resolut. Chromatogr.*, 2000, **23**, 93–99.
- 5 U. D. Neue, B. A. Alden, E. R. Grover, E. S. Grumbach, P. C. Iraneta and A. Méndez, in *Separation Science and Technology*, ed. A. Satinder and R. Henrik, Academic Press, 2007, vol. 8, pp. 45–83.
- 6 K. S. Mriziq, J. A. Abia, Y. Lee and G. Guiochon, *J. Chromatogr. A*, 2008, **1193**, 97–103.
- 7 P. D. I. Fletcher, S. J. Haswell, P. He, S. M. K. Kelly and A. Mansfield, *J. Porous Mater.*, 2011, **18**, 501–508.
- 8 P. He, S. J. Haswell, P. D. I. Fletcher, S. M. K. Kelly and A. Mansfield, *J. Flow Chem.*, 2012, **2**, 47–51.
- 9 R. A. Shalliker and H. Ritchie, *J. Chromatogr. A*, 2014, **1335**, 122–135.
- 10 J. P. Foley and J. G. Dorsey, *Anal. Chem.*, 1983, **55**, 730–737.
- 11 A. Soliven, G. R. Dennis, E. F. Hilder, R. A. Shalliker and P. G. Stevenson, *Chromatographia*, 2014, **77**, 663–671.

